

Superfluid Fraction in an Interacting Spatially Modulated Bose-Einstein Condensate

G. Chauveau, C. Maury, F. Rabec, C. Heintze, G. Brochier[✉], S. Nascimbene[✉], J. Dalibard[✉], and J. Beugnon^{✉*}
*Laboratoire Kastler Brossel, Collège de France, CNRS, ENS-PSL University,
 Sorbonne Université, 11 Place Marcelin Berthelot, 75005 Paris, France*

S. M. Roccuzzo and S. Stringari[†]
*Pitaevskii BEC Center, CNR-INO and Dipartimento di Fisica, Università di Trento,
 I-38123 Trento, Italy
 and Trento Institute for Fundamental Physics and Applications, INFN, 38123 Trento, Italy*

 (Received 3 February 2023; revised 7 April 2023; accepted 9 May 2023; published 2 June 2023)

At zero temperature, a Galilean-invariant Bose fluid is expected to be fully superfluid. Here we investigate theoretically and experimentally the quenching of the superfluid density of a dilute Bose-Einstein condensate due to the breaking of translational (and thus Galilean) invariance by an external 1D periodic potential. Both Leggett's bound fixed by the knowledge of the total density and the anisotropy of the sound velocity provide a consistent determination of the superfluid fraction. The use of a large-period lattice emphasizes the important role of two-body interactions on superfluidity.

DOI: [10.1103/PhysRevLett.130.226003](https://doi.org/10.1103/PhysRevLett.130.226003)

Superfluidity is a unique state of matter exhibited by quantum many-body systems in special conditions of temperature and interactions. It is characterized by the absence of viscosity and by many other peculiar phenomena, like the occurrence of quantized vortices, the reduction of the moment of inertia, the propagation of second sound at finite temperature, and Josephson effects. Superfluidity was first discovered in liquid helium [1,2]. More recently, an impressive amount of scientific activity has concerned the superfluid behavior of ultracold atomic gases (for a review, see Refs. [3–5]).

A key quantity characterizing superfluidity is the fraction of the total density, the so-called superfluid fraction, which determines superfluid transport phenomena. According to Landau's theory of superfluidity [6], at nonzero temperature the superfluid density does not coincide with the total density. The thermal occupation of elementary excitations provides the normal (nonsuperfluid) component responsible, for example, for the nonvanishing moment of inertia and the propagation of second sound [3]. The measurement of second sound velocity provides unique information on the temperature dependence of the superfluid density, in both liquid helium [7] and quantum gases [8,9].

At zero temperature, superfluid and total densities still do not always coincide, as illustrated by the celebrated superfluid to Mott-insulator transition [10–12]. Even in the mean-field regime relevant for the present work, consistent with the applicability of Gross-Pitaevskii theory, quenching of the superfluid density can occur when translation or Galilean invariances are broken, resulting in important consequences on the excitation spectrum. Such effects have been already pointed out theoretically in the presence

of disorder [13,14], external periodic potentials [15–20], supersolidity [21,22], and spin-orbit coupling [23–25]. Experimentally, the effects of the quenched superfluidity on the collective frequencies of a harmonically trapped gas were investigated in Ref. [26]. A similar situation emerges in astrophysics in the context of neutron stars where the periodic lattice of nuclei influences the superfluid density in the inner crust [27,28].

Here we provide a combined theoretical and experimental investigation of the reduction of the superfluid fraction caused by the presence of a periodic potential in a weakly interacting Bose-Einstein condensate (BEC) confined in a box. We determine the superfluid density employing Leggett's result [29,30], which is based on the knowledge of the *in situ* modulated total density profile $\rho(\mathbf{r})$, experimentally available thanks to the use of a large-period lattice. We also present an independent measurement of the superfluid fraction that exploits the anisotropic character of the sound velocity.

Superfluid fraction in a modulated potential.—We consider a two-dimensional (2D) weakly interacting BEC confined in a box of size $L \times L$, in the presence of the one-dimensional (1D) spatially periodic potential $V(x) = V_0 \cos(qx)$. This potential brings two energy scales to the problem, its amplitude V_0 and the “recoil energy” $\epsilon_q = \hbar^2 q^2 / 2m$, where m is the mass of an atom. Atomic interactions provide the third energy scale relevant for the problem. They are conveniently characterized by the chemical potential $\mu_0 = g\rho_0$ of a uniform condensate with a density equal to the average value $\rho_0 = \langle \rho(x) \rangle$, where $\rho(x)$ is the density profile and the average is calculated over one period of the potential $V(x)$. The interaction coupling

constant between atoms $g = 4\pi\hbar^2 a_s/m$ is fixed by the s -wave scattering length a_s .

In such a configuration, the superfluid fraction is an anisotropic rank-two tensor with eigenaxes x , y and with diagonal elements denoted $f_{s,\alpha}$ in the following ($\alpha = x, y$). They can be calculated by applying the perturbation $-v\hat{P}_\alpha$ to the system, where $\hat{P}_\alpha = \sum_{j=1}^N \hat{p}_{j,\alpha}$ is the momentum operator along the axis α , and N is the number of particles. This corresponds to working in the frame moving with velocity v with respect to the laboratory frame. Only the normal part reacts to the perturbation, so that, by calculating the average momentum $\langle \hat{P}_\alpha \rangle$ and imposing periodic boundary conditions, one accesses the superfluid fraction along the axis α ,

$$f_{s,\alpha} = 1 - \lim_{v \rightarrow 0} \frac{\langle \hat{P}_\alpha \rangle}{Nmv}. \quad (1)$$

A similar procedure, applied to the case of a rotating configuration, employing the angular momentum operator rather than the linear momentum operator, gives access to the moment of inertia, whose deviation from the rigid value provides direct evidence of superfluid effects [31].

In the presence of the periodic potential $V(x)$, the motion of the fluid is slowed down along the x direction, reflecting the quenching of the superfluid density along this direction: $\rho_{s,x} < \rho_0$. The superfluid density evaluated along the transverse y direction is instead not modified: $\rho_{s,y} = \rho_0$. The Gross-Pitaevskii equation (GPE) describing the weakly interacting BEC, solved in the frame moving with velocity v , i.e., subject to the constraint $-vP_x$, yields, according to the definition (1), the result [32]

$$f_{s,x} = \frac{\rho_{s,x}}{\rho_0} = \frac{1}{\langle \rho(x) \rangle \langle \frac{1}{\rho(x)} \rangle}. \quad (2)$$

According to the seminal work by Leggett [29,30], the right-hand side of (2) provides generally an upper bound to the superfluid density. Remarkably, the bound reduces to an identity in the case of a weakly interacting BEC subject to a 1D periodic potential [35].

Effective mass and sound propagation.—Result (2) may be surprising because it relates a transport property (the superfluid density) to a static quantity (the equilibrium density profile). The concept of effective mass, commonly used in the context of interacting Bose [16,19,37] and Fermi gases [20] placed in a periodic potential, elucidates this relation. In the present case, the superfluid fraction of the BEC, defined according to (2), exactly coincides with the ratio

$$\frac{m}{m_x^*} = f_{s,x}, \quad (3)$$

where the effective mass m_x^* fixes the curvature of the energy band along the x direction for small values of the quasimomentum (see Supplemental Material [32]).

The relation (3) between the effective mass and $f_{s,\alpha}$ illustrates the crucial role of the superfluid density in the propagation of sound. The hydrodynamic formalism of superfluids indeed provides the following expression for the velocity of a sound wave propagating along the x direction in the presence of $V(x)$ [3,16,26,38]:

$$c_x^2 = \frac{1}{m_x^* \kappa} = f_{s,x} \frac{1}{m\kappa}, \quad (4)$$

where $\kappa = [\rho_0 \partial_{\rho_0} \mu(\rho_0)]^{-1}$ is the compressibility of the gas. The value of the sound velocity propagating along the transverse y direction is

$$c_y^2 = \frac{1}{m\kappa}, \quad (5)$$

the effective mass m_y^* being equal to the bare mass in this case. The ratio between Eqs. (4) and (5) then provides

$$f_{s,x} = \frac{c_x^2}{c_y^2}. \quad (6)$$

The superfluid fraction can thus be determined either through the explicit knowledge of the equilibrium density profile via (2) or through the measurement of the ratio (6).

Limiting cases.—Results (2) and (6) hold for any values of the dimensionless parameters V_0/μ_0 and ϵ_q/μ_0 , as long as the description of the $T = 0$ Bose gas by a macroscopic wave function is valid, i.e., as long as quantum phase fluctuations between neighboring sites (a precursor of the superfluid to Mott-insulator transition) can be ignored. We now examine some limiting cases where $\rho(x)$ and $f_{s,x}$ take a simple expression.

We start with the very weakly interacting regime where $\mu_0 \ll \epsilon_q$. In this case, the GPE approaches the Schrödinger equation for a single particle subject to the periodic potential $V(x)$. In this regime, the identity $m^*/m = \langle \rho \rangle \langle 1/\rho \rangle$ was already noticed in Ref. [39].

The opposite case $\epsilon_q \ll \mu_0$ is described by the local density approximation (LDA). The validity condition of the LDA is equivalent to imposing that the period of the potential $2\pi/q$ be much larger than the healing length $\hbar/\sqrt{2mg\rho_0}$. In the LDA, the equilibrium density becomes $\rho^{(\text{LDA})}(x) = \rho_0 - \rho_1 \cos(qx)$ with $\rho_0 = \mu_0/g$ and $\rho_1 = V_0/g$. When injected into (2), this gives

$$f_{s,x}^{(\text{LDA})} = \left(1 - \frac{\rho_1^2}{\rho_0^2}\right)^{1/2} = \left(1 - \frac{V_0^2}{\mu_0^2}\right)^{1/2}. \quad (7)$$

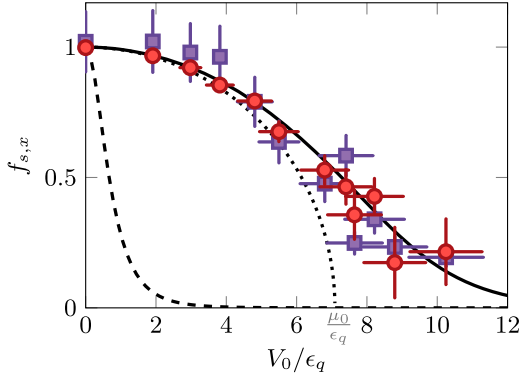


FIG. 1. Solid line: superfluid fraction calculated for a ^{87}Rb condensate by injecting the numerical solution of the GPE inside Leggett's formula (2) for $\rho_0 = 60 \mu\text{m}^{-2}$, $mg/\hbar^2 = 0.15$, and $2\pi/q = 3.93 \mu\text{m}$, corresponding to $\mu_0/\epsilon_q = 7.0$. Dotted line: LDA result. Red circles: experimental results obtained using Leggett's formula. Violet squares: experimental results obtained from speeds of sound. The dashed line shows the prediction in the opposite regime, $\mu_0 \ll \epsilon_q$, of a very weakly interacting system. In all figures, the error bar represents the statistical uncertainties of the measurements.

For values $V_0 > \mu_0$, the LDA density vanishes in a finite region within each period of $V(x)$, with the consequent vanishing of the superfluid fraction (dotted line in Fig. 1).

We now consider the third limiting case of small V_0 , which can be addressed using the formalism of the static density response function. An expansion of the solution of the GPE in powers of V_0 yields the amplitude of the first Fourier component of $\rho(x)$,

$$\frac{\rho_1}{\rho_0} = \frac{2V_0}{2\mu_0 + \epsilon_q} + \mathcal{O}(V_0^3). \quad (8)$$

Using (2), one finds the superfluid fraction [19]

$$f_{s,x} = 1 - \frac{2V_0^2}{(2\mu_0 + \epsilon_q)^2} + \mathcal{O}(V_0^4), \quad (9)$$

confirming the LDA result given above when we take the limit $\epsilon_q/\mu_0 \rightarrow 0$. Note that (8) and (9) also hold in the opposite limit of large ϵ_q/μ_0 , where the superfluid density no longer depends on the interaction.

The expansion of the solution of the GPE in powers of V_0 also provides the compressibility

$$\kappa = \mu_0^{-1} \left[1 - \frac{2V_0^2\epsilon_q}{(2\mu_0 + \epsilon_q)^3} \right] + \mathcal{O}(V_0^4), \quad (10)$$

showing that, different from the expansion (9) for the superfluid density, the V_0^2 correction to the compressibility vanishes in the LDA limit $\epsilon_q/\mu_0 \rightarrow 0$. In this limit, we thus predict from (4) and (5) that, at order 2 in V_0 , the speed of

sound c_y in the direction perpendicular to the lattice will not be affected by the presence of the lattice, whereas c_x will be reduced by an amount directly related to $f_{s,x}$.

The ideal gas limit.—The addition of a lattice on a Bose gas sheds interesting light on the controversial question of the possible superfluidity in the ideal case. The fact that the Landau criterion is not satisfied points to a nonsuperfluid character of the ideal gas, while the approach based on twisted boundary conditions leads to $f_s = 1$ for this system. To remove this ambiguity, we take a gas with chemical potential μ_0 placed in a lattice of large spatial period ($\epsilon_q \ll V_0$) and consider the two limits (i) $V_0 \rightarrow 0$ and (ii) $\mu_0 \rightarrow 0$. The order in which these limits are taken is crucial. If we take limit (i) first (i.e., $\epsilon_q \ll V_0 \ll \mu_0$) and then limit (ii), we find $f_s = 1$, see Eq. (9). Conversely, taking first the limit (ii) (i.e., $\epsilon_q, \mu_0 \ll V_0$) leads to $f_s \approx 0$ (see dashed line in Fig. 1). In our opinion, the latter approach is more relevant as it implicitly takes into account the residual (possibly disordered) modulated potentials acting on the gas.

Experimental setup.—We now describe the experimental determination of the superfluid fraction of a planar BEC subjected to a sinusoidal potential along x . The setup has been detailed in Refs. [40,41]. We start from a single quasi-2D Bose gas of ^{87}Rb atoms confined in an optical dipole trap made of a combination of repulsive laser beams at a wavelength $\lambda = 532 \text{ nm}$. We load all atoms around a single node of an optical lattice, which provides a strong confinement along the vertical direction z . It leads to an approximate harmonic confinement of frequency $\omega_z/2\pi \approx 3.7 \text{ kHz}$. The associated characteristic length $\ell_z = \sqrt{\hbar/m\omega_z} \approx 180 \text{ nm}$, is large compared to the s -wave scattering length $a_s = 5.3 \text{ nm}$, which leads to a quasi-2D regime where collisions keep their three-dimensional (3D) character. The effective 2D coupling constant describing the interactions in the cloud is $mg/\hbar^2 = \sqrt{8\pi}a_s/\ell_z \approx 0.15$. The 2D character of our gas is not crucial for this experiment, which could also be performed in a 3D boxlike potential [42].

The in-plane confinement is created by spatially shaped laser beams. A first beam creates a square box potential of size $L = 40 \mu\text{m}$. A second beam imposes the sinusoidal potential modulated along the x axis with a tunable amplitude V_0 from 0 to 80 nK [32,43]. The lattice period $d = 3.93(4) \mu\text{m}$ and the average 2D density $\rho_0 = 60(3) \mu\text{m}^{-2}$ are fixed. This corresponds to $\mu_0/k_B \approx 50 \text{ nK}$ and $\epsilon_q/k_B = 7.1 \text{ nK}$. The temperature of the gas is below the lowest measurable value in our setup, i.e., $< 20 \text{ nK}$.

Superfluid fraction from Leggett's formula.—To use Leggett's result (2), we measure the *in situ* 2D density profile $\rho^{(\text{meas})}(x, y)$ in the presence of the lattice using absorption imaging, see Fig. 2(a). We integrate it along y to obtain the 1D profile $\rho^{(\text{meas})}(x)$ [Fig. 2(b)]. For an ideal imaging system [44], $\rho^{(\text{meas})}(x) = \rho(x)$, but finite optical

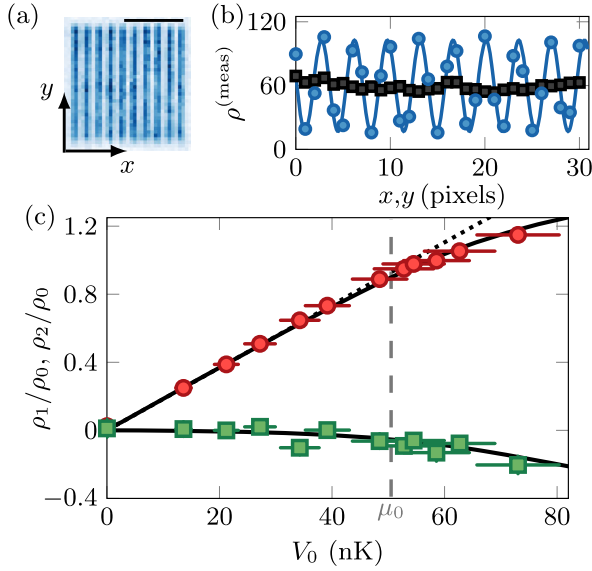


FIG. 2. (a) *In situ* absorption image of the 2D gas modulated with a lattice along x of period $3.93 \mu\text{m}$ and amplitude $V_0 = 54(5)$ nK. The length of the scale bar is $20 \mu\text{m}$. (b) Density profile integrated along x (squares) and y (circles) and the fit to a sinusoidal modulation (solid blue line) for $\rho^{(\text{meas})}(x)$. The pixel size is $1.15 \mu\text{m}$. (c) Fourier components of the density modulation ρ_n/ρ_0 versus the lattice depth V_0 for $n = 1$ (circles) and $n = 2$ (squares). Solid lines represent the corresponding predictions from the GPE. The dotted line is the weak lattice limit of (8).

resolution alters this relation and has to be included in the analysis. The expected density distribution can be expanded in Fourier series $\rho_0 - \sum_{n>0} \rho_n \cos(nqx)$, where the role of higher harmonics becomes increasingly important for large V_0 . We model our optical resolution by multiplicative coefficients $\beta_n < 1$: $\rho^{(\text{meas})}(x) = \rho_0 - \sum_{n>0} \beta_n \rho_n \cos(nqx)$.

We calibrate the first coefficients β_n by studying the density response to a lattice of wave number $q' = nq$ for low lattice depths. In this case, the density modulation $\rho(x)$ is dominated by its first harmonic and we fit the measured profiles to a sinusoidal function whose amplitude is adjusted to prediction (8). This adjustment provides $\beta_1 = 0.73(2)$ and $\beta_2 = 0.27(6)$, while the values of the coefficients $n \geq 3$ are below our experimental detectivity.

We show in Fig. 2(c) the values of $\rho_n = \rho_n^{(\text{meas})}/\beta_n$ for $n = 1, 2$. Both measurements are in good agreement with the predictions of the GPE (solid lines) over all the explored range of values of V_0 . From this measurement and restricting $\rho(x)$ to its two first Fourier components, we calculate Leggett's formula (2) and we plot the result as circles in Fig. 1. We discuss in the Supplemental Material [32] the effect of the truncation of the Fourier series on the solution of the GPE and confirm that, in our case, restricting to the first two harmonics already gives a good estimate of $f_{s,x}$.

Superfluid fraction from speed of sound.—We determine the speeds of sound along x and y by studying the response

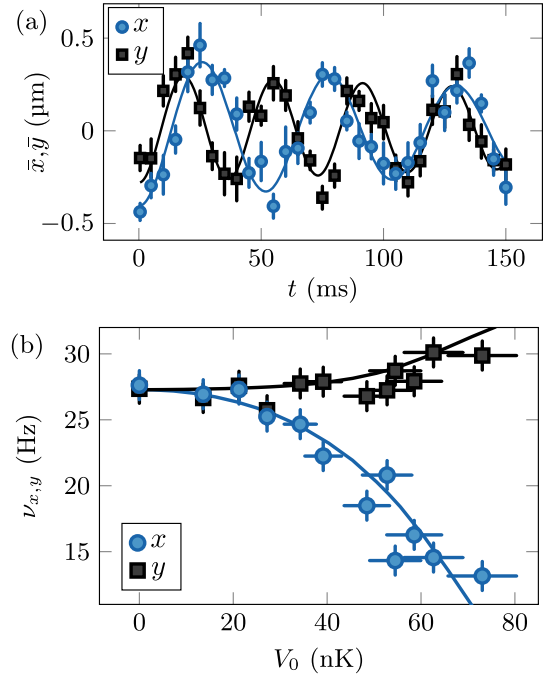


FIG. 3. Speed of sound measurement. (a) Center-of-mass position of the cloud after excitation as a function of time for an excitation along or perpendicular to the lattice for $V_0/k_B = 41(4)$ nK. The solid lines are sinusoidal fits to the data giving $\nu_x = 19(1)$ and $\nu_y = 27(1)$ Hz. (b) Extracted speed of sound along y (black squares) and x (blue circles) axes for different lattice depths. The solid lines are the prediction from the GPE.

of the cloud to an external perturbation of its density. Here, the perturbation consists of adding, during the preparation of the cloud, a weak linear magnetic potential along x or y , of amplitude ≈ 0.1 nK/ μm . At time $t = 0$, we abruptly switch off this potential and measure the evolution of the center of mass of the cloud, see Fig. 3(a). For a perturbation along x , we observe a smaller frequency than the one obtained for the same excitation along the y axis, a clear signature of the modification of the superfluid transport properties due to the presence of the lattice.

From the frequency $\nu_{x,y}$ of the fitted oscillations, we determine the speed of sound through the relation $c_{x,y} = 2L\nu_{x,y}$, valid when the lattice period and the healing length are both much smaller than the phonon wavelength, equal here to $2L$. We show our measurements in Fig. 3(b) as a function of the lattice depth. For a perturbation along y , we observe a small increase of c_y with V_0 , which can be attributed to the modification of the compressibility of the modulated gas with respect to the uniform case [see Eqs. (5) and (10)]. Along the axis of the lattice, we note a strong decrease of the speed of sound with the amplitude of the modulating potential, which we associate with the decrease of the superfluid fraction of the cloud. In addition, we plot with solid lines the result of a simulation of the

experimental protocol with the GPE. We observe an excellent agreement for both c_x and c_y . The superfluid fraction $f_{s,x}$ obtained from the ratio (6) is plotted in Fig. 1.

Discussion and conclusion.—The determination of the superfluid fraction $f_{s,x}$ based on sound propagation is in excellent agreement with the prediction from the GPE. The determination of $f_{s,x}$ based on Leggett’s formula, although limited by the finite resolution of our optical system, also agrees well with the prediction.

More generally, one may favor one of the two methods depending on the system under study. For example, in a spin-orbit coupled BEC that violates Galilean invariance [25], the sound velocity measurement will give access to the superfluid fraction, while the density may remain uniform, in which case Leggett’s bound is not relevant. Conversely, in supersolid BECs [45–51], the excitation spectrum is, in general, more complex [52,53] and the sound velocity measurement is not directly applicable to extract f_s , which, at least in one-dimensional-like configurations, may be instead calculated using Leggett’s formula [54]. A challenging question concerns the determination of the superfluid density in higher dimensions if the total density profile is not factorizable along the various directions [30], as in the case of 2D dipolar supersolids [50] and of a vortex lattice [55]. Our Letter also paves the way for the investigation of the superfluid fraction in other density modulated quantum gases, like Fermi superfluids and 1D and disordered systems. It could be extended to study the links between the quenching of the superfluid fraction and the emergence of number squeezing and phase fluctuations effects [17,56] for deep periodic potentials, as well as to investigate the consequence of finite temperature effects.

We acknowledge the support by ERC (Grant Agreement No. 863880) and ANR (Grant Agreement No. ANR-18-CE30-0010). We thank Brice Bakkali-Hassani for his participation at the early stage of the project. We also acknowledge Tony Leggett, Anne-Laure Dalibard, Stefano Giorgini, Augusto Smerzi, Alessio Recati, Christopher Pethick, and Ian Spielman for fruitful discussions.

G. C., C. M., and F. R. contributed equally to this work.

Note added.—Recently, a manuscript by Tao *et al.* explored anisotropic superfluidity in a periodically modulated trapped BEC gas [57]. We employ here lattices with much larger periods, allowing for an explicit measurement of Leggett’s formula and enhancing the role of two-body interactions.

*beugnon@lkb.ens.fr

†sandro.stringari@unitn.it

[1] P. Kapitza, Viscosity of liquid helium below the λ -point, *Nature (London)* **141**, 74 (1938).

- [2] J. F. Allen and A. D. Misener, Flow of liquid helium II, *Nature (London)* **141**, 74 (1938).
- [3] L. Pitaevskii and S. Stringari, *Bose-Einstein Condensation and Superfluidity* (Oxford University Press, New York, 2016).
- [4] C. J. Pethick and H. Smith, *Bose-Einstein Condensation in Dilute Gases* (Cambridge University Press, Cambridge, 2008).
- [5] A. J. Leggett, *Quantum Liquids: Bose Condensation and Cooper Pairing in Condensed-Matter Systems* (Oxford University Press, New York, 2006).
- [6] L. Landau, Theory of the superfluidity of helium II, *Phys. Rev.* **60**, 356 (1941).
- [7] V. P. Peshkov, Second sound in He II, *J. Phys. Moscow* **8**, 131 (1944).
- [8] L. A. Sidorenkov, M. K. Tey, R. Grimm, Y.-H. Hou, L. Pitaevskii, and S. Stringari, Second sound and the superfluid fraction in a Fermi gas with resonant interactions, *Nature (London)* **498**, 78 (2013).
- [9] P. Christodoulou, M. Galka, N. Dogra, R. Lopes, J. Schmitt, and Z. Hadzibabic, Observation of first and second sound in a Berezinskii-Kosterlitz-Thouless superfluid, *Nature (London)* **594**, 191 (2021).
- [10] M. P. A. Fisher, Peter B. Weichman, G. Grinstein, and Daniel S. Fisher, Boson localization and the superfluid-insulator transition, *Phys. Rev. B* **40**, 546 (1989).
- [11] D. Jaksch, C. Bruder, J. I. Cirac, C. W. Gardiner, and P. Zoller, Cold Bosonic Atoms in Optical Lattices, *Phys. Rev. Lett.* **81**, 3108 (1998).
- [12] M. Greiner, O. Mandel, T. Esslinger, T. W. Hänsch, and I. Bloch, Quantum phase transition from a superfluid to a Mott insulator in a gas of ultracold atoms, *Nature (London)* **415**, 39 (2002).
- [13] S. Giorgini, L. Pitaevskii, and S. Stringari, Effects of disorder in a dilute Bose gas, *Phys. Rev. B* **49**, 12938 (1994).
- [14] C. Gaul, N. Renner, and C. A. Müller, Speed of sound in disordered Bose-Einstein condensates, *Phys. Rev. A* **80**, 053620 (2009).
- [15] J. Javanainen, Phonon approach to an array of traps containing Bose-Einstein condensates, *Phys. Rev. A* **60**, 4902 (1999).
- [16] M. Krämer, L. Pitaevskii, and S. Stringari, Macroscopic Dynamics of a Trapped Bose-Einstein Condensate in the Presence of 1D and 2D Optical Lattices, *Phys. Rev. Lett.* **88**, 180404 (2002).
- [17] A. Smerzi, A. Trombettoni, P. G. Kevrekidis, and A. R. Bishop, Dynamical Superfluid-Insulator Transition in a Chain of Weakly Coupled Bose-Einstein Condensates, *Phys. Rev. Lett.* **89**, 170402 (2002).
- [18] M. Machholm, C. J. Pethick, and H. Smith, Band structure, elementary excitations, and stability of a Bose-Einstein condensate in a periodic potential, *Phys. Rev. A* **67**, 053613 (2003).
- [19] E. Taylor and E. Zaremba, Bogoliubov sound speed in periodically modulated Bose-Einstein condensates, *Phys. Rev. A* **68**, 053611 (2003).
- [20] G. Watanabe, G. Orso, F. Dalfovo, L. P. Pitaevskii, and S. Stringari, Equation of state and effective mass of the unitary Fermi gas in a one-dimensional periodic potential, *Phys. Rev. A* **78**, 063619 (2008).

- [21] S. Saccani, S. Moroni, and M. Boninsegni, Excitation Spectrum of a Supersolid, *Phys. Rev. Lett.* **108**, 175301 (2012).
- [22] T. Macrì, F. Maucher, F. Cinti, and T. Pohl, Elementary excitations of ultracold soft-core bosons across the superfluid-supersolid phase transition, *Phys. Rev. A* **87**, 061602(R) (2013).
- [23] Y. Li, G. I. Martone, L. P. Pitaevskii, and S. Stringari, Superstripes and the Excitation Spectrum of a Spin-Orbit-Coupled Bose-Einstein Condensate, *Phys. Rev. Lett.* **110**, 235302 (2013).
- [24] G. I. Martone, Y. Li, L. P. Pitaevskii, and S. Stringari, Anisotropic dynamics of a spin-orbit-coupled Bose-Einstein condensate, *Phys. Rev. A* **86**, 063621 (2012).
- [25] Y.-C. Zhang, Z.-Q. Yu, T. K. Ng, S. Zhang, L. Pitaevskii, and S. Stringari, Superfluid density of a spin-orbit-coupled Bose gas, *Phys. Rev. A* **94**, 033635 (2016).
- [26] F. S. Cataliotti, S. Burger, C. Fort, P. Maddaloni, F. Minardi, A. Trombettoni, A. Smerzi, and M. Inguscio, Josephson junction arrays with Bose-Einstein condensates, *Science* **293**, 843 (2001).
- [27] N. Chamel, Neutron conduction in the inner crust of a neutron star in the framework of the band theory of solids, *Phys. Rev. C* **85**, 035801 (2012).
- [28] G. Watanabe and C. J. Pethick, Superfluid Density of Neutrons in the Inner Crust of Neutron Stars: New Life for Pulsar Glitch Models, *Phys. Rev. Lett.* **119**, 062701 (2017).
- [29] A. J. Leggett, Can a Solid be “Superfluid”?, *Phys. Rev. Lett.* **25**, 1543 (1970).
- [30] A. J. Leggett, On the superfluid fraction of an arbitrary many-body system at $T = 0$, *J. Stat. Phys.* **93**, 927 (1998).
- [31] S. Stringari, Moment of Inertia and Superfluidity of a Trapped Bose Gas, *Phys. Rev. Lett.* **76**, 1405 (1996).
- [32] See Supplemental Material at <http://link.aps.org/supplemental/10.1103/PhysRevLett.130.226003> for complementary theoretical discussions and experimental details, which includes Refs. [33,34].
- [33] C. Dorrer and J. D. Zuegel, Design and analysis of binary beam shapers using error diffusion, *J. Opt. Soc. Am. B* **24**, 1268 (2007).
- [34] L. Corman, J. L. Ville, R. Saint-Jalm, M. Aidelsburger, T. Bienaimé, S. Nascimbène, J. Dalibard, and J. Beugnon, Transmission of near-resonant light through a dense slab of cold atoms, *Phys. Rev. A* **96**, 053629 (2017).
- [35] Result (2) for the superfluid density does not hold only in the presence of periodic potentials of the form $V_0 \cos(qx)$. For example, it provides the Josephson energy in the presence of a junction separating two BECs [36].
- [36] I. Zapata, F. Sols, and A. J. Leggett, Josephson effect between trapped Bose-Einstein condensates, *Phys. Rev. A* **57**, R28 (1998).
- [37] W. Zwerger, Mott–Hubbard transition of cold atoms in optical lattices, *J. Opt. B* **5**, S9 (2003).
- [38] A. Bensoussan, J.-L. Lions, and G. Papanicolaou, *Asymptotic Analysis for Periodic Structures* (American Mathematical Society, Providence, 2011), Vol. 374.
- [39] A. J. Leggett (private communication).
- [40] J. L. Ville, T. Bienaimé, R. Saint-Jalm, L. Corman, M. Aidelsburger, L. Chomaz, K. Kleinlein, D. Perconte, S. Nascimbène, J. Dalibard, and J. Beugnon, Loading and compression of a single two-dimensional Bose gas in an optical accordion, *Phys. Rev. A* **95**, 013632 (2017).
- [41] J. L. Ville, R. Saint-Jalm, É. Le Cerf, M. Aidelsburger, S. Nascimbène, J. Dalibard, and J. Beugnon, Sound Propagation in a Uniform Superfluid Two-Dimensional Bose Gas, *Phys. Rev. Lett.* **121**, 145301 (2018).
- [42] A. L. Gaunt, T. F. Schmidutz, I. Gotlibovych, R. P. Smith, and Z. Hadzibabic, Bose-Einstein Condensation of Atoms in a Uniform Potential, *Phys. Rev. Lett.* **110**, 200406 (2013).
- [43] Y.-Q. Zou, É. Le Cerf, B. Bakkali-Hassani, C. Maury, G. Chauveau, P. C. M. Castilho, R. Saint-Jalm, S. Nascimbène, J. Dalibard, and J. Beugnon, Optical control of the density and spin spatial profiles of a planar Bose gas, *J. Phys. B* **54**, 08LT01 (2021).
- [44] We use a weakly saturating imaging beam and partial transfer imaging to image low density clouds and stay in the linear absorption regime.
- [45] J. Léonard, A. Morales, P. Zupancic, T. Esslinger, and T. Donner, Supersolid formation in a quantum gas breaking a continuous translational symmetry, *Nature (London)* **543**, 87 (2017).
- [46] J.-R. Li, J. Lee, W. Huang, S. Burchesky, B. Shteynas, F. C. Top, A. O. Jamison, and W. Ketterle, A stripe phase with supersolid properties in spin-orbit-coupled Bose-Einstein condensates, *Nature (London)* **543**, 91 (2017).
- [47] L. Chomaz, D. Petter, P. Ilzhöfer, G. Natale, A. Trautmann, C. Politi, G. Durastante, R. M. W. van Bijnen, A. Patscheider, M. Sohmen, M. J. Mark, and F. Ferlaino, Long-Lived and Transient Supersolid Behaviors in Dipolar Quantum Gases, *Phys. Rev. X* **9**, 021012 (2019).
- [48] F. Böttcher, J.-N. Schmidt, M. Wenzel, J. Hertkorn, M. Guo, T. Langen, and T. Pfau, Transient Supersolid Properties in an Array of Dipolar Quantum Droplets, *Phys. Rev. X* **9**, 011051 (2019).
- [49] L. Tanzi, E. Lucioni, F. Famà, J. Catani, A. Fioretti, C. Gabbanini, R. N. Bisset, L. Santos, and G. Modugno, Observation of a Dipolar Quantum Gas with Metastable Supersolid Properties, *Phys. Rev. Lett.* **122**, 130405 (2019).
- [50] M. A. Norcia, C. Politi, L. Klaus, E. Poli, M. Sohmen, M. J. Mark, R. N. Bisset, L. Santos, and F. Ferlaino, Two-dimensional supersolidity in a dipolar quantum gas, *Nature (London)* **596**, 357 (2021).
- [51] L. Tanzi, J. G. Maloberti, G. Biagioni, A. Fioretti, C. Gabbanini, and G. Modugno, Evidence of superfluidity in a dipolar supersolid from nonclassical rotational inertia, *Science* **371**, 1162 (2021).
- [52] C. Josserand, Y. Pomeau, and S. Rica, Patterns and supersolids, *Eur. Phys. J. Spec. Top.* **146**, 47 (2007).
- [53] J. Hofmann and W. Zwerger, Hydrodynamics of a superfluid smectic, *J. Stat. Mech.* (2021) 033104.
- [54] S. Rocuzzo, Supersolidity in a dipolar quantum gas, Ph.D. thesis, Università di Trento, 2021.
- [55] E. B. Sonin, Vortex oscillations and hydrodynamics of rotating superfluids, *Rev. Mod. Phys.* **59**, 87 (1987).
- [56] C. Orzel, A. K. Tuchman, M. L. Fenselau, M. Yasuda, and M. A. Kasevich, Squeezed states in a Bose-Einstein condensate, *Science* **291**, 2386 (2001).
- [57] J. Tao, M. Zhao, and I. Spielman, Observation of anisotropic superfluid density in an artificial crystal, [arXiv:2301.01258](https://arxiv.org/abs/2301.01258).